DOI:10.1021/jf900041j

JOURNAL OF AGRICULTURAL AND FOOD CHEMISTRY
ARTICLE

Functional Proteomic Analysis Predicts Beef Tenderness and the Tenderness Differential

Isain Zapata, Henry N. Zerby, and Macdonald Wick*

Department of Animal Sciences, The Ohio State University, Columbus, Ohio 43210

Inconsistent tenderness is one of the most detrimental factors of meat quality. Functional proteomics was used to associate electrophoretic bands from the myofibrillar muscle fraction to meat tenderness in an effort to gain understanding of the mechanisms controlling tenderness. The myofibrillar muscle fraction of the *Longissimus dorsi* from 22 Angus cross steers was analyzed by SDS-PAGE and linearly regressed to Warner−Bratzler shear values. Six significant electrophoretic bands were characterized by electrophoretic and statistical analysis and sequenced by nano-LC-MS/MS. The protein(s)/peptide(s) identified in these bands encompass a wide array of cellular pathways related to structural, metabolic, chaperone, and developmental functions. This study begins to assemble information that has been reported separately into a more complete picture that will lead to the establishment of a coherent mechanism accounting for meat tenderness.

KEYWORDS: Beef; *Longissimus dorsi*; proteomics; tenderness

INTRODUCTION

Tenderness is considered to be one of the most important of all the organoleptic characteristics contributing to meat quality (*1*). Recent reports (*2*−*5*) highlight the inability of the current USDA beef quality grading system to accurately segregate carcasses into tenderness categories, and these reports stress the importance of tenderness characteristics to overall beef quality. This quality inconsistency results in consumers being dissatisfied with the beef products currently available at the retail and food service level (*3*), with consumers indicating that they would pay a premium for beef of known tenderness (*6*).

The mechanisms controlling meat tenderness involve a multitude of cellular functions, which have proven difficult to develop into a coherent model. Variations in genetics (*7*), final pH (*8*), the cathepsins, the calpain/calpastatin system, the proteasome (*9*), collagen content, collagen cross-linking, myofibrillar degradation (*10*), and, more recently, heat shock proteins (*11*, *12*) are thought to play roles in the mechanisms controlling tenderness. It is likely that all of these processes participate, to some extent, in the mechanisms resulting in beef carcass tenderness.

A novel approach to gain understanding of the mechanisms controlling tenderness and to predict tenderness is by elucidating the state of the muscle cell through the use of functional proteomics, which is a combination of electrophoretic, image, statistical, and protein sequencing technologies that identifies the protein(s)/peptide(s) associated with Warner−Bratzler shear (WBS), a common method of assessing beef tenderness (*13*, *14*).

Therefore, the objective of the present study was to perform a functional proteomic analysis to associate electrophoretic bands from the myofibrillar fraction of meat samples at 36 h postmortem that are statistically significant with meat tenderness at 72 h and 14 days of aging and/or the tenderness differential and determine the sequence of the protein(s)/peptide(s) in those bands.

*Corresponding author [telephone (614) 292-7516; e-mail wick.13@osu.edu].

MATERIALS AND METHODS

Experimental Design. The selection of the two time points for WBS was designed to capture two different scenarios of post-mortem aging, which are the nonaged meat phase, represented by the 72 h time point, and the aged meat phase, represented by the 14 day time point. Samples for proteomic analysis were taken at 36 h.

Animals and Sample Collection. Twenty-two Angus crossbred steers with no Brahman influence, of approximately 18 months of age, were harvested in the abattoir at The Ohio State University Meat Laboratory following USDA-accepted welfare practices. No electrical stimulation was performed. All muscle samples were taken from the eighth rib region of the *Longissimus dorsi* muscle. Samples for proteomic analysis were taken from one side of the carcass at 36 h, and steak samples for tenderness value determination by WBS were taken at 72 h and 14 days post-mortem (during cold-room aging) were taken from the other. Samples destined for proteomic analysis were flash frozen in liquid nitrogen and stored at −20 °C.

Warner−Bratzler Shear Force Analysis. Steaks aged for 72 h or 14 days were cooked on a cooking grill (George Foreman Next Grilleration; Salton, Inc., Miramar, FL) set to 190.5 °C and cooked to an internal temperature of 71.1 °C monitored with a scanning thermocouple thermometer (Digi-Sense 12-Channel Benchtop Thermocouple Scanner; Barnant Co., Barrington, IL). The cooked steaks were then cooled to room temperature, and six cores, 1.27 cm in diameter, were sampled parallel to the muscle fiber orientation. Shear force values of the cores were obtained using a TA-XT Plus Texturometer (Stable Micro Systems Ltd., Godalming, U.K.). The average WBS value of the six cores was calculated and used as the shear force value for the samples.

Proteomic Analysis. A myofibrillar fraction of each muscle sample was prepared by homogenizing 250 mg of muscle for 1 min with 3 mL of a low-salt buffer [50 mM NaCl, 0.1% NaN_3 0.4 mM Pefabloc SC Plus, (Boehringer Mannheim Corp., Indianapolis, IN), pH 7.2] on ice.

 Published on Web 05/18/2009

The homogenate was centrifuged at 10000*g* for 10 min. The supernatant was discarded, and the resulting myofibril pellet was suspended in 2 mL of low-salt buffer and centrifuged at 10000*g* for 10 min. This step was repeated three times. The supernatant was discarded, and the 50 mg pellet (myofibrillar fraction) was dissolved in sample buffer (8 M urea/2 M thiourea, 75 mM DTT, 50 mM Tris, 3% SDS, and 0.004% bromophenol blue, pH 6.8) at a ratio of 1 mg of sample per 30 μL of sample buffer. The samples were then incubated on ice for 30 min. Samples were centrifuged at 10000*g* for 10 min prior to loading onto a 1 mm × 12 cm × 14 cm polyacrylamide slab gel consisting of 10−20% gradient resolving gel [30:0.8, acrylamide/*N*,*N*′-bis(methylene acrylamide)] and a 3% stacking gel containing 1% SDS. Electrophoretic separation was carried out at a constant voltage of 10 V cm^{-1}. After electrophoretic separation, gels were placed in fixing solution (50% methanol, 7% acetic acid) for 12 h and then stained with SYPRO Ruby protein gel stain (Bio-Rad Laboratories, Inc., Hercules, CA) for 24 h protected from light. The gels were then placed in destain solution (10% methanol, 7% acetic acid) for 30 min and rinsed with deionized water prior to imaging. The gels were scanned using a Typhoon 9400 laser scanner (GE Healthcare, Chalfont St. Giles, U.K.) using the SYPRO Ruby setting, but with the 457 nm blue laser. Digital images were analyzed using the Total Lab TL120 (Nonlinear Dynamics Inc., Newcastle upon Tyne, U.K.) software. The bands were identified and then analyzed to determine the percentage contribution of each band in relation to the total band volume in the lane.

Statistical Analysis. A multiple linear regression model previously developed and published (*14*) was fitted using the dependent variables. The percent contribution of each band, obtained from Total Lab TL120, in each lane was imported into SAS v.9.1.3 (SAS Institute Inc., Cary, NC) for subsequent multiple linear regression analysis. This model consists of a stepwise multiple linear regression within the REG procedure of SAS. In a stepwise model, bands are removed or added iteratively from the model in each step of the procedure according to their significance ($P = 0.05$ was used in this study) starting with a model that includes no bands and ending with a model that includes all bands that meet the significance criteria. The purpose of the model is to determine which bands from the proteomic analysis were contributing to the variation of the dependent variable as described below:

$$Y_i = \beta_0 + \beta_j X_{ij} + \varepsilon_{ij}$$

where Y_i is the dependent variable measured of the ith sample ($i = 1, ..., n$), β_0 is the intercept, β_j is the regression parameter associated with the jth band ($j = 1, ..., 30$), X_{ij} is the percent contribution for the jth band of the ith sample, and ε_{ij} is the random error inherent to each sample, which is assumed to be independent and normally distributed.

Band Sequencing. The bands that were determined by the multiple linear regression model as being predictive of the dependent variable were submitted for characterization by mass spectrometry as previously described (*14*) with the following modifications. The associated bands from three animals that showed the highest values of the dependent variable were pooled together and were analyzed as one; the same procedure was performed with the associated bands from three animals that showed the lowest values of the dependent variable. All mass spectrometry was performed at the Campus Chemical Instrument Center of The Ohio State University using established methods. Briefly, selected bands were excised from the gel, washed in 50% methanol/5% acetic acid solution, and dehydrated in acetonitrile. Gel bands were rehydrated and incubated with 5 mg/mL of DTT in 100 mM ammonium bicarbonate solution prior to the addition of 15 mg/mL iodoacetamide in 100 mM ammonium bicarbonate solution. Gel bands were washed with acetonitrile and ammonium bicarbonate (100 mM) and were dried in a speed vac; the protease is driven into the gel pieces by rehydrating them in 50 μL of sequencing grade modified trypsin (Promega, Madison, WI), and the mixture was incubated at 25 °C overnight. Peptides were extracted from the polyacrylamide with a 50% acetonitrile/5% formic acid solution. The extracted pools were concentrated in a speed vac to ~30 μL. Pools were analyzed by capillary liquid chromatography−nanospray tandem mass spectrometry (nano-LC-MS/MS) performed on a Thermo Finnigan LTQ mass spectrometer equipped with a nanospray source operated in positive ion mode. The LC system was an UltiMate Plus system (Dionex Co., Sunnyvale, CA) with a Famos autosampler and Switchos column switcher. Solvent A was water containing 50 mM acetic acid, and solvent B was acetonitrile. Five microliters of each sample were eluted into a 5 cm, 75 μm ID. ProteoPep II C18 column (New Objective, Inc., Woburn, MA) packed directly in the nanospray tip. Peptides were eluted directly off the column into the LTQ system using a gradient of 2−80% solvent B over 50 min, with a flow rate of 300 nL/min. The scan sequence of the mass spectrometer was based on the TopTen method; the analysis was programmed for a full scan recorded between 350 and 2000 Da and a MS/MS scan to generate product ion spectra to determine amino acid sequence in consecutive instrument scans of the 10 most abundant peaks in the spectrum. Sequence information from the MS/MS data were searched using Mascot Daemon v.2.2.1 (Matrix Science, Boston, MA) and the database searched against the full Swiss-Prot database v.55.3 (366,226 sequences; 132,054,191 residues). The mass accuracy of the precursor ions was set to 2.0 Da given that the data were acquired on an ion trap mass analyzer and the fragment mass accuracy was set to 0.5 Da. Modifications considered were methionine oxidation and carbamidomethyl cysteine. Two missed cleavages for the enzyme were permitted. Protein identifications were checked manually.

Sequencing Result Interpretation. The two main confounders that complicate the interpretation of mass spectrometry data are that the identified sequences can be found on multiple sequences found in the database and proteins/peptides can comigrate in bands resolved by one-dimensional SDS-PAGE. Because of this, the list of protein sequences found in each band sequenced had to be trimmed to facilitate our interpretation. The criteria employed to trim the list was as follows: (1) Remove all identified sequences from trypsin (the protease used to digest the bands) and keratin (a common contaminant of samples that comes from the contact of skin with the device or its components). (2) Remove all sequences identified from non-bovine sources. (3) Remove all sequences when significance was based on only one fragment significantly identified. This is a common practice, because single fragment identifications can lead to misinterpretations (*15*).

RESULTS AND DISCUSSION

It has been previously shown that electrophoretic analyses at 36 h post-mortem can be used to predict tenderness at 7 days (*13*). It is likely that this is true for 72 h tenderness and 14 day tenderness, as well. The descriptive statistics of the WBS values, and the change from 72 h WBS to 14 day WBS (ΔWBS), are presented in **Table 1**. ΔWBS was used to estimate the tenderness differential between those two time points. As expected, WBS force values declined from 72 h to 14 days post-mortem, which can also be observed in the mean ΔWBS, which has a negative value. One-way ANOVA supported the difference in WBS force values between the two time points ($P < 0.001$).

Functional Proteomic Analysis of Myofibrils. Functional proteomics relies on statistically analyzing the variation of the staining intensities of bands in an electrophoretic profile. This allows for identification of bands that are significantly associated with a dependent variable. In this study, that variable was WBS or tenderness. The protein(s)/peptide(s) present in the bands were sequenced by tandem mass spectrometry.

Thirty protein/peptide bands across all samples were electrophoretically resolved and matched across all samples by Total Lab TL120. A representative gel, comparison of an animal for which the maximum value of the dependent variable was observed to an animal for which the minimum value was observed is shown in **Figure 1**. In some of the cases the differences can be

Table 1. Descriptive Statistics for Warner−Bratzler Shear Force (WBS)[a]

dependent variable	*n*	mean (N)	SD (N)	min (N)	max (N)	range (N)
72 h WBS	22	53.37	12.58	37.06	75.82	38.76
14 day WBS	22	36.69	6.38	26.98	51.85	24.87
ΔWBS	22	−16.68	12.37	−40.99	4.45	45.44

[a] Δ refers to the dynamic change over time (ΔWBS = 14 day WBS − 72 h WBS).

spotted by the naked eye; however, it is enhanced by the software. The synthetic lane is shown in **Figure 2** along with the estimated molecular weights. The synthetic lane is an artificial reference lane that contains all of the bands separated through all samples and allows band matching across samples. To avoid the confounding factor of uneven protein loading, the percentage that each band contributed to the total staining of all bands within the lane was estimated by the software. This value was determined from the integration of the intensity of each peak in the electropherogram after background removal.

Intact actin and myosin band images were removed from further analyses following the recommendation of previous literature (*13*). To generate quantifiable bands of the proteins/peptides present in muscle, other than actin and myosin, it was necessary to load sufficient sample to maximize the number of resolvable bands as determined by the image analysis software; this resulted in overloading of actin and myosin. Thus, this overloading of actin and myosin meant that the linear increases in the amount of sample loaded did not result in a linear increase in the band intensities of actin or myosin. This discrepancy would prevent quantifying the loss of these proteins during the aging process. In any case, linear losses of these two proteins during aging would be observed in other quantifiable bands.

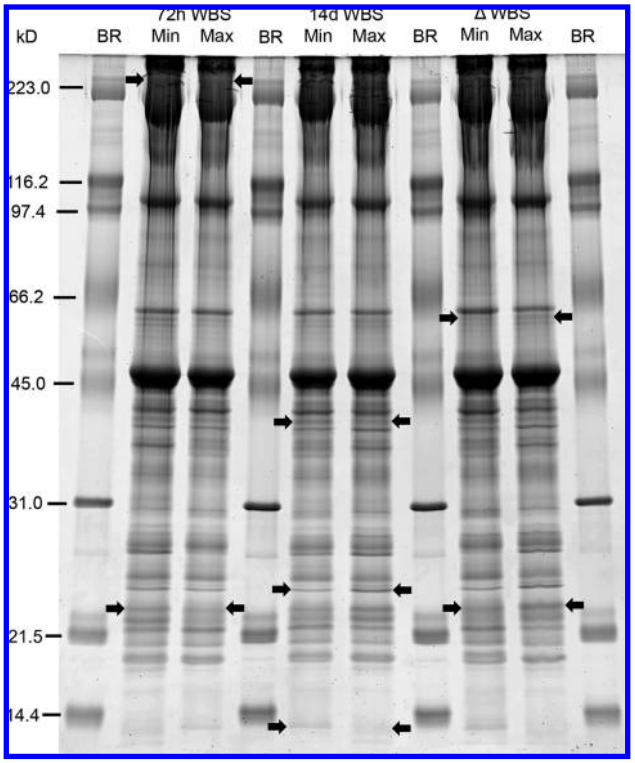

Figure 1. Comparative 10−20% gradient SDS-PAGE gel showing the samples for which the minimum (Min) and maximum (Max) value for the respective dependent variable (72 h WBS, 14 day WBS, and ΔWBS) were observed. The arrows show the location of the bands found to be significantly associated with the dependent variable. BR is the broad range molecular weight marker.

The multiple linear regression models were fitted using the dependent variables previously discussed (72 h WBS, 14 day WBS, and ΔWBS), and the bands that were found to be significant for each multiple linear regression were identified. Three separate multiple linear regressions were fitted, and the equations obtained were

$$72\text{ h WBS} = 57.044 + 2.652(\text{band 2}) - 9.678(\text{band 25})$$

$$(R^2 = 0.508; P < 0.001; \text{SEM} = 9.276\text{ N})$$

$$14\text{ day WBS} = 19.738 + 1.105(\text{band 12}) + 4.134(\text{band 24}) - 2.902(\text{band 30})$$

$$(R^2 = 0.674; P < 0.001; \text{SEM} = 3.934\text{ N})$$

$$\Delta\text{WBS} = -23.074 - 18.455(\text{band 9}) + 10.768(\text{band 25})$$

$$(R^2 = 0.576; P < 0.001; \text{SEM} = 8.472\text{ N})$$

One band (band 25) was found to be significantly predictive for two of the dependent variables. No band was found to be predictive for all three variables. A total of six bands were identified in this study.

It should be noted that in the case of 72 h WBS and 14 day WBS, a positive regression coefficient in a specific band means that, as the band intensity increases, the WBS value increases, which translates to less tender meat. Thus, a negative regression coefficient will describe the opposite phenomenon; if the band intensity increases, the WBS value decreases, which results in more tender meat. In the case of ΔWBS, the interpretation is different; if the regression coefficient is positive, it indicates a smaller WBS differential, which translates to a lesser range of tenderization during aging. As well, a negative regression coefficient indicates larger WBS differential, which indicates a greater range of tenderization during aging.

Band Sequencing and Protein Identification. The three highest and three lowest most extreme samples, for each of the dependent variables, were selected for sequencing. This was done to normalize the animal-to-animal variation, thus avoiding the observation

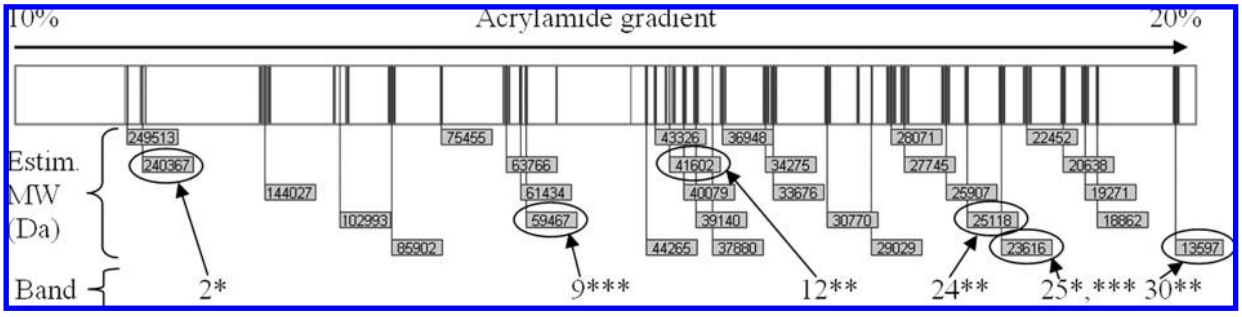

Figure 2. Representation of the synthetic lane used to align and compare the SDS-PAGE profiles. The 30 resolved bands are displayed. Estimated molecular weights (MW) were calculated using the broad range standard. The bands found to be associated are circled. *, band associated with 72 h WBS; **, band associated with 14 day WBS; ***, band associated with ΔWBS.

Table 2. Comparison of Individual Samples To Be Pooled Together for Band Sequencing[a]

dependent variable	level	individual WBS (N)	pooled WBS (mean) (N)
7 h WBS	H	74.32, 75.46, 75.82	75.20
	L	37.06, 40.33, 40.53	39.31
14 day WBS	H	45.51, 49.66, 51.85	49.01
	L	26.98, 30.84, 30.97	29.60
ΔWBS	H	−5.22, −3.20, 4.45	−1.32
	L	−40.99,−34.78, −34.70	−36.82

[a] The three samples that showed the highest (H) and lowest (L) values for each dependent variable were combined for sequencing.

of results from a single animal. Details of the selected samples are displayed in **Table 2**. The six bands found to be predictive of and associated with WBS force values were cut from the gel to be sequenced. The Mascot Daemon software sequencing identification process blasts the peptide sequences found in the band against the Swiss-Prot protein database for matching against known protein sequences. The software sorts the results on the basis of the statistical significance of the identification. Only results found to be significant ($P \leq 0.05$) are considered. The significance is determined by the summation of the probability of each fragment identified and matched to that specific sequence, which is expressed as a score value (MOWSE score).

The protein sequences identified using these criteria are presented in **Tables 3**−**5**, on the basis of the dependent variable analyzed. Thirty-six individual proteins/peptides were identified, although many of the same proteins/peptides were identified in more than one band. This may be due to proteolytic fragments of the intact protein comigrating in a band of lower molecular weight than that of the intact protein. It was also observed, in **Table 3**, that in band 2 myosin heavy chain comigrated along with myosin light chain 2 at an estimated molecular weight of ∼240 kDa even though myosin light chain 2 has a molecular weight of ∼19 kDa. It is generally accepted that both myosin light and heavy chains are associated via non-covalent bonding. In some cases, proteins comigrated in bands with larger molecular weights. This phenomenon has been shown to occur with myosin heavy chain due to the covalent cross-linking activity of transglutaminase in the muscle (*16*). The same phenomenon has also been observed in vitro with troponin T (*17*). Our observation suggests that a covalent association between the two molecules is formed post-mortem.

In this study, we identified protein(s)/peptide(s) that have structural, metabolic, chaperone, and/or developmental functions that appear to be participating, in unison, in the mechanism of meat tenderness. The limitation of our study resides in the comigration of protein(s)/peptide(s) within a given band that confound the ability to definitively identify which protein(s)/peptide(s) are involved with a biological mechanism or pathway. Therefore, we were unable to definitively identify which protein(s)/peptide(s) were playing a direct role in the mechanisms underlying post-mortem tenderness, but several trends are apparent.

One trend was the presence of structural proteins specific to the sarcomere. Both intact and proteolytic fragments of myosin heavy chains, in bands 2 and 9, and myosin light chains, in bands 2, 24, 25, and 30, tended to be found in bands associated with all WBS variables. Myosin heavy chains and myosin light chains are crucial to muscle function in terms of contraction velocity and power that is associated with fiber type composition. Fiber type composition is based on the myosin heavy chain and myosin light chain isoform composition which, ultimately, determines the main source of energy for the muscle (*18*). This observation supports the notion that the muscle fiber type composition is related, in some way, to the post-mortem proteolytic events that may lead to meat tenderization. These results are also consistent with recent reports on meat tenderness. Muscle fiber type is associated with tenderness in Angus and Brahman crossbreeds (*19*). Post-mortem concentrations of both myosin heavy chain fragments and myosin light chain 1 have been associated with pork quality and tenderness (*20*, *21*) and beef tenderness (*13*). In addition, recent reports in cattle have shown that bovine myosin light chain 1 is fragmented soon after harvest and that the fragment increases 11-fold by 24 h postharvest (*22*). Additionally, both 1D and 2D electrophoresis experiments have shown that myosin heavy chain is proteolyzed by μ-calpain (*20*).

Another trend was the presence of the structural protein actin with a molecular weight higher than 40 kDa in band 9 that was found to be negatively associated with ΔWBS. Thus, the presence of actin migrating at a higher molecular weight than the full molecular weight suggests it is covalently bound to a myosin fragment migrating at a lower molecular weight than its reported value of 223 kDa. It is interesting to speculate that this phenomenon is fiber-type specific. Myosin binds to actin to perform its biological function of muscle contraction. Muscle contraction

Table 3. Sequencing Data of Bands Associated with 72 h WBS[a]

band [MWe[b] (kDa)]	association type[c]	identification	Swiss-Prot accession no.	MOWSE scores[d] (H/L)	fragments identified[e] (H/L)	MWt[f] (kDa)
2 (240.4)	+	myosin heavy chain 1	MYH1_BOVIN	5672/6451	272/341	223.76
		myosin heavy chain 2	MYH2_BOVIN	5647/6100	257/328	224.09
		myosin heavy chain 7	MYH7_BOVIN	3552/4095	165/196	223.89
		sarcoplasmic reticulum calcium ATPase 1	AT2A1_BOVIN	229/284	5/7	110.53
		myosin light chain 2, skeletal	MLRS_BOVIN	0/76	0/3	19.11
25 (23.6)	−	myosin light chain 2, skeletal	MLRS_BOVIN	929/895	43/37	19.11
		myosin light chain 2, ventricular	MLRV_BOVIN	580/406	29/16	18.97
		heat shock protein β 6	HSPB6_BOVIN	144/146	5/5	17.51
		creatine kinase M type	KCRM_BOVIN	130/105	5/2	43.19
		troponin C, slow skeletal and cardiac	TNNC1_BOVIN	120/0	3/0	18.52
		crystalline α B chain	CRYAB_BOVIN	47/0	2/0	20.02

[a] The comparison between the pooled sample of animals with high 72 h WBS values (H) versus the pooled sample of animals with low 72 h WBS (L) values is displayed. [b] MWe is the experimental molecular weight. [c] Type of association with the dependent variable. [d] The MOWSE score is a numeric descriptor of the likelihood that the identification is correct. [e] Number of fragments sequenced and matched to that particular protein. [f] MWt is the theoretical molecular weight.

Table 4. Sequencing Data of Bands Associated with 14 Day WBS[a]

band [MWe[b] (kDa)]	association type[c]	identification	Swiss-Prot accession no.	MOWSE scores[d] (H/L)	fragments identified[e] (H/L)	MWt[f] (kDa)
12 (41.6)	+	tropomyosin β chain	TPM2_BOVIN	1006/1286	46/49	32.93
		creatine kinase M type	KCRM_BOVIN	784/886	42/43	43.19
		actin α, skeletal	ACTS_BOVIN	724/724	44/42	42.37
		tropomyosin α 3 chain	TPM3_BOVIN	546/459	22/19	32.86
		glyceraldehyde 3 phosphate dehydrogenase	G3P_BOVIN	210/226	5/7	36.07
		aspartate aminotransferase, mitochondrial	AATM_BOVIN	133/135	4/2	47.88
		creatine kinase, sarcomeric	KCRS_BOVIN	116/0	3/0	47.71
		glyceraldehyde 3 phosphate dehydrogenase, testis	G3PT_BOVIN	0/94	0/2	43.66
24 (25.1)	+	crystalline α B chain	CRYAB_BOVIN	488/347	18/11	20.02
		nyosin light chain 2, skeletal	MLRS_BOVIN	221/154	8/8	19.11
		creatine kinase M type	KCRM_BOVIN	215/0	6/0	43.19
		actin α, skeletal	ACTS_BOVIN	94/0	4/0	42.37
		cysteine and glycine-rich protein 3	CSRP3_BOVIN	62/0	2/0	21.85
30 (13.6)	−	myosin light chain 1, skeletal	MLE1_BOVIN	568/604	24/30	21.03
		hemoglobin subunit β	HBB_BOVIN	442/487	14/15	16.00
		histone H4	H4_BOVIN	239/337	9/13	11.36
		cytochrome C oxidase subunit 5A, mitochondrial	COX5A_BOVIN	185/245	6/8	16.90
		myosin light chain 2, skeletal	MLRS_BOVIN	96/0	4/0	19.11
		cytochrome B-C1 complex subunit 7	QCR7_BOVIN	77/0	3/0	13.47
		galectin 1	LEG1_BOVIN	0/229	0/7	15.08
		ATP synthase subunit E, mitochondrial	ATP5I_BOVIN	0/121	0/3	8.32
		hemoglobin subunit α 1/2	HBA_BOVIN	0/88	0/5	15.18
		ATP synthase subunit F, mitochondrial	ATPK_BOVIN	0/59	0/2	10.34
		glyceraldehyde 3 phosphate dehydrogenase, testis	G3PT_BOVIN	0/54	0/2	43.66

[a] The comparison between the pooled sample of animals with high 14 day WBS values (H) versus the pooled sample of animals with low 14 day WBS (L) values is displayed. [b] MWe is the experimental molecular weight. [c] Type of association with the dependent variable. [d] The MOWSE score is a numeric descriptor of the likelihood that the identification is correct. [e] Number of fragments sequenced and matched to that particular protein. [f] MWt is the theoretical molecular weight.

can be observed post-mortem during rigor onset. The actomyosin bond requires the binding of ATP to return the structure to the relaxed state. Post-mortem actomyosin release is limited by ATP availability. This availability has been reported to be dependent on fiber-type composition (*23*). It can also be due to transglutaminase activity as described before.

Research has shown that degradation of the structural proteins desmin and troponin T is also correlated with increased tenderness in beef (*24*) and lamb (*25*) during aging. In the present study, desmin was identified in band 9 migrating at an estimated molecular weight of 59 kDa, which is close to its intact molecular weight of 52 kDa. Even though troponin T was not identified in any of the bands in this study, another member of the troponin complex, troponin C, was identified in band 25 at∼22 kDa and was negatively associated with 72 h WBS and positively associated with ΔWBS; the protein migrated close to its reported full-length molecular weight of ∼19 kDa.

Another trend was the observation in all six statistically significant bands of at least one enzyme involved in energy metabolism. Overall, the metabolic enzymes identified were several ATP synthase subunits, a pair of creatine kinase isoforms, a mitochondrial aspartate aminotransferase isoform, two different glyceraldehyde 3 phosphate dehydrogenase isoforms, one cytochrome B-C1 subunit, one cytochrome C oxidase subunit, and an oxoglutarate dehydrogenase component. An important point to note is the presence of these proteins in the myofibrillar fraction. Creatine kinase and glyceraldehyde 3 phosphate dehydrogenase are soluble proteins that are normally found in the low-salt soluble sarcoplasmic fraction of muscle tissue. Precipitation of these proteins in the myofibrillar fraction may be the result of higher temperatures and lower pH conditions present in post-mortem tissue, as suggested by research performed on pork (*26*, *27*). We do not have an explanation for this phenomenon. It is possible that these peptides were trapped interstitially during the extraction process or that these proteins were precipitated by isoelectric precipitation (*27*). The presence of fragments of these sarcoplasmic proteins is likely due to proteolytic events occurring during the aging process as we are not aware of pH being capable of fragmenting of proteins in post-mortem conditions.

Previous research found that increased metabolism immediately post-mortem resulted in higher WBS values and less tender meat and that inhibiting glycolysis resulted in increased tenderness and lower WBS values (*28*). In that study, the addition of glycolytic inhibitors to enhance tenderness was studied. Muscles that were treated with glycolytic inhibitors were more tender, with lower WBS, than muscles that received a control treatment. Additionally, it has been shown that tenderness is enhanced with decreased glycolytic activity due to the activity of the calpain system, which has been shown to be more active at a pH closer to physiological levels (*29*). However, reduced glycolytic potential naturally within muscle is generally accepted to not lead to increased tenderness. Rather, the opposite has been shown to occur. In one study, muscle with decreased glycolytic potential was more likely to exhibit a dark, firm, and dry (DFD) condition. The DFD beef was less tender and had more off-flavors than beef from muscles with increased glycolytic potential (*30*). It is likely that post-mortem energy metabolism plays an undefined, yet critical, role in determining beef tenderness.

One more trend was the presence of participation of the heat shock protein or chaperone β 6 (Hspβ6) in band 25. Heat shock proteins have been included in recent studies involving meat tenderness. One of those studies, in beef, found a negative relationship between tenderness and heat shock protein 40 (Hsp40), a protein that helps to retard cell death in muscle

Table 5. Sequencing Data of Bands Associated with the Change from 72 h WBS to 14 Day WBS (ΔWBS)[a]

band [MWe[b] (kDa)]	association type[c]	identification	Swiss-Prot accession no.	MOWSE scores[d] (H/L)	fragments identified[e] (H/L)	MWt[f] (kDa)
9 (59.5)	−	myosin heavy chain 2	MYH2_BOVIN	2031/812	82/26	224.09
		myosin heavy chain 1	MYH1_BOVIN	1919/753	77/27	223.76
		desmin	DESM_BOVIN	1447/634	62/22	53.56
		ATP synthase subunit α, heart	ATPA1_BOVIN	1160/1358	42/49	59.80
		myosin heavy chain 7	MYH7_BOVIN	712/292	23/13	223.89
		tubulin β 2C chain	TBB2C_BOVIN	290/342	12/11	50.26
		tubulin β 3 chain	TBB3_BOVIN	228/0	11/0	50.86
		actin α, skeletal	ACTS_BOVIN	224/456	7/17	42.37
		ATP synthase subunit β, mitochondrial	ATPB_BOVIN	131/372	4/11	52.25
		creatine kinase M type	KCRM_BOVIN	62/0	3/0	43.19
		tubulin α 3 chain	TBA3_BOVIN	54/0	2/0	50.59
		tubulin α 4A chain	TBA4A_BOVIN	0/91	0/2	50.63
		dihydrolipoyllysine-residue succinyltransferase component of 2-oxoglutarate dehydrogenase complex, mitochondrial	ODO2_BOVIN	0/60	0/3	49.28
25 (23.6)	+	myosin light chain 2, ventricular	MLRV_BOVIN	762/618	40/33	18.97
		myosin light chain 2, skeletal	MLRS_BOVIN	666/854	27/42	19.11
		troponin C, slow skeletal and cardiac	TNNC1_BOVIN	245/226	8/6	18.52
		heat shock protein β 6	HSPB6_BOVIN	230/48	10/2	17.51
		crystalline α B chain	CRYAB_BOVIN	215/162	7/5	20.02
		cysteine and glycine-rich protein 3	CSRP3_BOVIN	155/0	5/0	21.85

[a] The comparison between the pooled sample of animals with high ΔWBS values (H) versus the pooled sample of animals with low ΔWBS (L) values is displayed. [b] MWe is the experimental molecular weight. [c] Type of association with the dependent variable. [d] The MOWSE score is a numeric descriptor of the likelihood that the identification is correct. [e] Number of fragments sequenced and matched to that particular protein. [f] MWt is the theoretical molecular weight.

tissue (*11*). In another study, it was reported that heat shock protein 27 (Hsp27) was down-regulated in animals that gave lower tenderness values (*12*). Results of our study associated Hspβ6 with tenderness variability. Hspβ6 is alternatively known as heat shock protein 20 (Hsp20) (*31*) and has been described as having a strong affinity to actin thin filaments in muscle tissues and to be highly homologous to Hsp27 (*32*).

Hsp20 has been related to muscle relaxation during high calcium concentration events during situations of acute stress (*33*). In our study, Hspβ6 was shown to be negatively associated with 72 h WBS and positively associated with Δ WBS, which is consistent with the literature (*12*). It seems reasonable to assume that the function of Hsp20 is comparable to the function of Hsp27, which is intimately related to the stability of the actin thin filament based on the fact that the sequence elements responsible for their activity are highly conserved between the two (*33*, *34*). Thus, it seems reasonable to postulate that alterations in the regulation of Hspβ6 may lead to decreased stability of the actin filament, which may be associated with increased tenderness (*12*).

The presence of Hspβ6 in the myofibrillar fraction and has to do with the conditions of the extraction process. We used a low-salt solution adjusted to a pH of 7.2. A relevant difference from other small heat shock proteins is that Hspβ6 is not soluble in a pH ranging from 6 to 8 (this range includes the pH of our solution) Its difference in solubility from other similar heat shock proteins is suspected to be related to subcellular specialization (*35*). Hspβ6's singular solubility explains its presence in our myofibrillar preparation.

A trend, unique to our study, related tenderness to muscle differentiation. The cysteine and glycine-rich protein 3 (found in band 24), also known as muscle LIM, was found to be positively associated with 14 day WBS. The muscle LIM protein contains the LIM domain, which is a cysteine−histidine rich, zinc-coordinating domain, consisting of two tandemly repeated zinc fingers. The proteins called LIM contain the LIM domain. The LIM domain takes its name from *L*in11, *I*sl-1, and *M*ec-3 proteins, in which the domain was first discovered (*36*). This protein functions as a positive developmental regulator that works as a cofactor of MyoD, MRF4, and myogenin to promote myoblast terminal differentiation (*37*). The RNA expression of this protein has been observed to be increased in muscle tissue of beef cattle undergoing nutritional stress (*38*), but this is the first report of its link to tenderness. The presence of this protein indicates that the muscle is undergoing hyperplasic growth, which leads to an increased cell number that requires additional structural scaffolding leading to perimysium accumulation. LIM was also positively associated with ΔWBS (band 25). The additional structural scaffolding required for supporting the increased cell numbers may be sufficient to offset the proteolytic breakdown that occurs post-mortem, which is reflected by a smaller WBS differential.

This idea is further supported by the presence of α and β tubulin isoforms in band 9, which are specific to microtubules. Microtubules provide structural support that helps maintain the shape of cells. Recently, microtubules have been reported to be apoptotic targets (*39*, *40*) of caspases and granzyme B. The participation of apoptotic pathways in muscular post-mortem metabolism related to meat tenderization has been previously suggested (*9*).

Finally, both α and β hemoglobin subunits were identified in band 30, which was negatively associated with ΔWBS. This observation is interesting because a correlation of hemoglobin concentration in meat and tenderness variation has not been previously reported. With regard to meat quality, preslaughter hemoglobin concentration in blood has been studied for prediction of carcass color (*41*, *42*). In the same manner, there were also other protein(s)/peptide(s) identified in the bands; however, their relationship with meat tenderness has never been reported or suggested. As mentioned before, the electrophoretic comigration of protein(s)/peptide(s) currently confounds our ability to quantify the protein(s)/peptide(s) that identify the direct participants involved in the mechanism of meat tenderization.

Conclusion. In our study, WBS values were observed to be associated with the structural proteins, myosin heavy chains, myosin light chains, actin, desmin, and tubulin or their fragments. Our results are consistent with previous reports showing that degradation of thick filament components at 36 h is predictive of future tenderness in beef (*13*). Finding structural proteins that were predictive of tenderness in this study supports a hypothesis previously suggested (*43*, *44*) that the architecture within the myofibril in post-mortem muscle may be an important contributor to the eventual tenderness after aging due to the weakening of the actomyosin interaction during post-mortem proteolysis.

Besides the participation of structural proteins in meat tenderization processes, proteins with metabolic, developmental, and chaperone functions have also been identified. The participation of metabolic enzymes in meat tenderization can be easily related to muscle fiber type composition; however, proteins with developmental or chaperone functions are harder to relate.

By identifying the mechanisms through which tenderness is mediated, it will be possible to develop more precise breeding strategies to produce cattle with greater and more consistent tenderness. This study identified multiple proteins that have been previously reported in separate studies that are related to meat tenderization. The methodology used in this study has the potential to capture the participants of multiple processes in a single experiment. The results of this study begin, for the first time, to assemble those proteins into participants in a coherent mechanism underlying the tenderization process.

LITERATURE CITED

(1) Koohmaraie, M. The role of Ca(2+)-dependent proteases (calpains) in post mortem proteolysis and meat tenderness. *Biochimie* **1992**, *74* (3), 239–245.

(2) Smith, G. C., Savell, J. W., Dolezal, H. G., Field, T. G., Gill, D. R., Griffin, D. B., Hale, D. S., Morgan, J. B., Northcutt, S. L., Tatum, J. D. Improving the quality, consistency, competitiveness and market-share of beef. *The Final Report of the Second Blueprint for Total Quality Management in the Fed-Beef (Slaughter Steer/Heifer) Industry. National Beef Quality Audit − 1995*; National Cattleman's Beef Association: Englewood, CO, 1996.

(3) Brooks, J. C.; Belew, J. B.; Griffin, D. B.; Gwartney, B. L.; Hale, D. S.; Henning, W. R.; Johnson, D. D.; Morgan, J. B.; Parrish, F. C.Jr; Reagan, J. O.; Savell, J. W. National Beef Tenderness Survey—1998. *J. Anim. Sci.* **2000**, *78* (7), 1852–1860.

(4) Roeber, D. L., Belk, K. E., Savell, J. W., Morgan, J. B., Montgomery, T. H., Smith, G. C. In What are the "top ten quality challenges" for the U.S. fed-beef industry; consensus of the participants in phase III, the strategy workshop, of the national beef quality audit − 2000. *The Final Report of the Third Blueprint for Total Quality Management in the Fed-Beef (Slaughter Steer/Heifer) Industry. National Beef Quality Audit − 2000*; National Cattleman's Beef Association: Englewood, CO, 2001.

(5) McKenna, D. R.; Roebert, D. L.; Bates, P. K.; Schmidt, T. B.; Hale, D. S.; Griffin, D. B.; Savell, J. W.; Brooks, J. C.; Morgan, J. B.; Montgomery, T. H.; Belk, K. E.; Smith, G. C. National Beef Quality Audit−2000: survey of targeted cattle and carcass characteristics related to quality, quantity, and value of fed steers and heifers. *J. Anim. Sci.* **2002**, *80* (5), 1212–1222.

(6) Boleman, S. J.; Boleman, S. L.; Miller, R. K.; Taylor, J. F.; Cross, H. R.; Wheeler, T. L.; Koohmaraie, M.; Shackelford, S. D.; Miller, M. F.; West, R. L.; Johnson, D. D.; Savell, J. W. Consumer evaluation of beef of known categories of tenderness. *J. Anim. Sci.* **1997**, *75* (6), 1521–1524.

(7) Dikeman, M. E.; Pollak, E. J.; Zhang, Z.; Moser, D. W.; Gill, C. A.; Dressler, E. A. Phenotypic ranges and relationships among carcass and meat palatability traits for fourteen cattle breeds, and heritabilities and expected progeny differences for Warner−Bratzler shear force in three beef cattle breeds. *J. Anim. Sci.* **2005**, *83* (10), 2461–2467.

(8) Shackelford, S. D.; Koohmaraie, M.; Cundiff, L. V.; Gregory, K. E.; Rohrer, G. A.; Savell, J. W. Heritabilities and phenotypic and genetic correlations for bovine postrigor calpastatin activity, intramuscular fat content, Warner-Bratzler shear force, retail product yield, and growth rate. *J. Anim. Sci.* **1994**, *72* (4), 857–863.

(9) Ouali, A.; Herrera-Mendez, C. H.; Coulis, G.; Becila, S.; Boudjellal, A.; Aubry, L.; Sentandreu, M. A. Revisiting the conversion of muscle into meat and the underlying mechanisms. *Meat Sci.* **2006**, *74* (1), 44–58.

(10) Sifre, L.; Berge, P.; Engel, E.; Martin, J. F.; Bonny, J. M.; Listrat, A.; Taylor, R.; Culioli, J. Influence of the spatial organization of the perimysium on beef tenderness. *J. Agric. Food Chem.* **2005**, *53*, 8390–8399.

(11) Bernard, C.; Cassar-Malek, I.; Le Cunff, M.; Dubroeucq, H.; Renand, G.; Hocquette, J. F. New indicators of beef sensory quality revealed by expression of specific genes. *J. Agric. Food Chem.* **2007**, *55*, 5229–5237.

(12) Morzel, M.; Terlouw, C.; Chambon, C.; Micol, D.; Picard, B. Muscle proteome and meat eating qualities of *Longissimus thoracis* of "Blonde d'Aquitaine" young bulls: a central role of HSP27 isoforms. *Meat Sci.* **2008**, *78* (3), 297–304.

(13) Sawdy, J. C.; Kaiser, S. A.; St-Pierre, N. R.; Wick, M. P. Myofibrillar 1-D fingerprints and myosin heavy chain MS analyses of beef loin at 36 h postmortem correlate with tenderness at 7 days. *Meat Sci.* **2004**, *67* (3), 421–426.

(14) Reddish, J. M.; St-Pierre, N.; Nichols, A.; Green-Church, K.; Wick, M. Proteomic analysis of proteins associated with body mass and length in yellow perch, *Perca flavescens*. *Proteomics* **2008**, *8* (11), 2333–2343.

(15) Wilkins, M. R.; Appel, R. D.; Eyk, J. E. V.; Chung, M. C. M.; Gorg, A.; Hecker, M.; Huber, L. A.; Langen, H.; Link, A. J.; Paik, Y.-K.; Patterson, S. D.; Pennington, S. R.; Rabilloud, T.; Simpson, R. J.; Weiss, W.; Dunn, M. J. Guidelines for the next 10 years of proteomics. *Proteomics* **2006**, *6* (1), 4–8.

(16) Eligula, L.; Chuang, L.; Phillips, M. L.; Motoki, M.; Seguro, K.; Muhlrad, A. Transglutaminase induced cross-linking between subdomain 2 of G-actin and the 636−642 lysine-rich loop of myosin subfragment 1. *Biophys. J.* **1998**, *74* (2), 953–963.

(17) Bergamini, C. M.; Signorini, M.; Barbato, R.; Menabo, R.; Dilisa, F.; Gorza, L.; Beninati, S. Transglutaminase catalyzed polymerization of troponin in vitro. *Biochem. Biophys. Res. Commun.* **1995**, *206* (1), 201–206.

(18) Bottinelli, R. Functional heterogeneity of mammalian single muscle fibres: do myosin isoforms tell the whole story?. *Pflugers Arch.* **2001**, *443* (1), 6–17.

(19) Stolowski, G. D.; Baird, B. E.; Miller, R. K.; Savell, J. W.; Sams, A. R.; Taylor, J. F.; Sanders, J. O.; Smith, S. B. Factors influencing the variation in tenderness of seven major beef muscles from three Angus and Brahman breed crosses. *Meat Sci.* **2006**, *73* (3), 475–483.

(20) Lametsch, R.; Roepstorff, P.; Moller, H. S.; Bendixen, E. Identification of myofibrillar substrates for u-calpain. *Meat Sci.* **2004**, *68*, 515–521.

(21) Lametsch, R.; Karlsson, A.; Rosenvold, K.; Andersen, H. J.; Roepstorff, P.; Bendixen, E. Postmortem proteome changes of porcine muscle related to tenderness. *J. Agric. Food Chem.* **2003**, *51*, 6992–6997.

(22) Jia, X.; Hollung, K.; Therkildsen, M.; Hildrum, K. I.; Bendixen, E. Proteome analysis of early post-mortem changes in two bovine muscle types: M. longissimus dorsi and M. semitendinosis. *Proteomics* **2006**, *6* (3), 936–944.

(23) Bowker, B. C.; Botrel, C.; Swartz, D. R.; Grant, A. L.; Gerrard, D. E. Influence of myosin heavy chain isoform expression and postmortem metabolism on the ATPase activity of muscle fibers. *Meat Sci.* **2004**, *68*, 587–594.

(24) Ho, C. Y.; Stromer, M. H.; Rouse, G.; Robson, R. M. Effects of electrical stimulation and postmortem storage on changes in titin, nebulin, desmin, troponin-T, and muscle ultrastructure in *Bos indicus* crossbred cattle. *J. Anim. Sci.* **1997**, *75* (2), 366–376.

(25) Wheeler, T. L.; Koohmaraie, M. The extent of proteolysis is independent of sarcomere length in lamb longissimus and psoas major. *J. Anim. Sci.* **1999**, *77* (9), 2444–2451.
(26) Fischer, C.; Hamm, R. Biochemical studies on fast glycolysing bovine muscle. *Meat Sci.* **1979**, 41–49.
(27) Joo, S. T.; Kauffman, R. G.; Kim, B. C.; Park, G. B. The relationship of sarcoplasmic and myofibrillar protein solubility to colour and water-holding capacity in porcine longissimus muscle. *Meat Sci.* **1999**, *52* (3), 291–297.
(28) Jerez, N. C.; Calkins, C. R.; Velazco, J. Prerigor injection using glycolytic inhibitors in low-quality beef muscles. *J. Anim. Sci.* **2003**, *81* (4), 997–1003.
(29) Beltrán, J. A.; Jaime, I.; Santolaria, P.; Sañudo, C.; Albertí, P.; Roncalés, P. Effect of stress-induced high post-mortem pH on protease activity and tenderness of beef. *Meat Sci.* **1997**, *45* (2), 201–207.
(30) Wulf, D. M.; Emnett, R. S.; Leheska, J. M.; Moeller, S. J. Relationships among glycolytic potential, dark cutting (dark, firm, and dry) beef, and cooked beef palatability. *J. Anim. Sci.* **2002**, *80* (7), 1895–1903.
(31) Kappé, G.; Franck, E.; Verschuure, P.; Boelens, W. C.; Leunissen, J. A.; Jong, W. W. d. The human genome encodes 10 α-crystallin-related small heat shock proteins: HspB1−10. *Cell Stress Chaperon* **2003**, *8* (1), 53–61.
(32) Kato, K.; Goto, S.; Inaguma, Y.; Hasegawa, K.; Morishita, R.; Asano, T. Purification and characterization of a 20-kDa protein that is highly homologous to α B Crystallin. *J. Biol. Chem.* **1994**, *269* (21), 15302–15309.
(33) Rembold, C. M.; Foster, D. B.; Strauss, J. D.; Wingard, C. J.; Van Eyk, J. E. cGMP-mediated phosphorylation of heat shock protein 20 may cause smooth muscle relaxation without myosin light chain dephosphorylation in swine carotid artery. *J. Physiol.* **2000**, *524* (3), 865–878.
(34) Guay, J.; Lambert, H.; Gingras-Breton, G.; Lavoie, J. N.; Huot, J.; Landry, J. Regulation of actin filament dynamics by p38 map kinase-mediated phosphorylation of heat shock protein 27. *J. Cell. Sci.* **1997**, *110* (3), 357–368.
(35) Quraishe, S.; Asuni, A.; Boelens, W. C.; O'Connor, V.; Wyttenbach, A. Expression of the small heat shock protein family in the mouse CNS: differential anatomical and biochemical compartmentalization. *Neuroscience* **2008**, *153* (2), 483–491.
(36) Bach, I. The LIM domain: regulation by association. *Mech. Dev.* **2000**, *91* (1−2), 5–17.
(37) Kong, Y.; Flick, M. J.; Kudla, A. J.; Konieczny, S. F. Muscle LIM protein promotes myogenesis by enhancing the activity of MyoD. *Mol. Cell. Biol.* **1997**, *17* (8), 4750–4760.
(38) Lehnert, S. A.; Byrne, K. A.; Reverter, A.; Nattrass, G. S.; Greenwood, P. L.; Wang, Y. H.; Hudson, N. J.; Harper, G. S. Gene expression profiling of bovine skeletal muscle in response to and during recovery from chronic and severe undernutrition. *J. Anim. Sci.* **2006**, *84* (12), 3239–3250.
(39) Adrain, C.; Duriez, P. J.; Brumatti, G.; Delivani, P.; Martin, S. J. The cytotoxic lymphocyte protease, granzyme B, targets the cytoskeleton and perturbs microtubule polymerization dynamics. *J. Biol. Chem.* **2006**, *281* (12), 8118–8125.
(40) Moss, D. K.; Betin, V. M.; Malesinski, S. D.; Lane, J. D. A novel role for microtubules in apoptotic chromatin dynamics and cellular fragmentation. *J. Cell. Sci.* **2006**, *119* (11), 2362–2374.
(41) Wilson, L. L.; Egan, C. L.; Henning, W. R.; Mills, E. W.; Drake, T. R. Effects of live animal performance and hemoglobin level on special-fed veal carcass characteristics. *Meat Sci.* **1995**, *41* (1), 89–96.
(42) Klont, R. E.; Barnier, V. M.; van Dijk, A.; Smulders, F. J.; Hoving-Bolink, A. H.; Hulsegge, B.; Eikelenboom, G. Effects of rate of pH fall, time of deboning, aging period, and their interaction on veal quality characteristics. *J. Anim. Sci.* **2000**, *78* (7), 1845–1851.
(43) Goll, D. E.; Geesink, G. H.; Taylor, R. G.; Thompson, V. F. Does proteolysis cause all postmortem tenderization, or are changes in the actin/myosin interaction involved?. *Proc. Int. Congr. Meat Sci. Technol.* **1995**, *41*, 537–544.
(44) Goll, D. E.; Boehm, M. L.; Geesink, G. H.; Thompson, V. F. What causes postmortem tenderization? *Proc. 50th Annu. Reciprocal Meats Conf.* **1998**, 60−67 Appendix A.

Received January 5, 2009. Revised manuscript received April 1, 2009. This project was funded in part by the OARDC Graduate Research Enhancement Grant Program.